Letter

Hydrodynamics of electron-hole fluid photogenerated in a mesoscopic two-dimensional channel

M. A. T. Patricio,[1] G. M. Jacobsen,[2] M. D. Teodoro,[2] G. M. Gusev,[3] A. K. Bakarov,[4] and Yu. A. Pusep[1,*]

[1]*São Carlos Institute of Physics, University of São Paulo, P.O. Box 369, 13560-970 São Carlos, São Paulo, Brazil*

[2]*Departamento de Física, Universidade Federal de São Carlos, 13565-905 São Carlos, São Paulo, Brazil*

[3]*Institute of Physics, University of São Paulo, 135960-170 São Paulo, São Paulo, Brazil*

[4]*Institute of Semiconductor Physics, 630090 Novosibirsk, Russia*

(Received 14 September 2023; revised 14 February 2024; accepted 14 February 2024; published 6 March 2024)

The dynamics of the diffusion flow of holes photoinjected into a mesoscopic GaAs channel of variable width, where they, together with background electrons, form a hydrodynamic electron-hole fluid, is studied using time-resolved microphotoluminescence. It is found that the rate of recombination of photoinjected holes, which is proportional to the rate of their flow, decreases when holes pass through the expanded sections of the channel. In fact, this is the Venturi effect, which consists in a decrease in the velocity of the fluid in the expanded sections of the pipe. Moreover, a nonuniform diffusion velocity profile is observed, similar to the parabolic Hagen-Poiseuille velocity profile, which indicates a viscous hydrodynamic flow. It is shown that in agreement with a theory, the magnetic field strongly suppresses the viscosity of the electron-hole fluid. Additional evidence of the viscous nature of the studied electron-hole fluid is the observed increase in the recombination rate with increasing temperature, which is similar to the decrease in the electrical resistance of viscous electrons with temperature.

DOI: 10.1103/PhysRevB.109.L121401

Introduction. For almost three decades, the hydrodynamics of electron systems has continued to be one of the most attractive problems in solid state physics. The history of the hydrodynamic approach in condensed matter physics is well described in Ref. [1]. The hydrodynamic theory is based only on the conservation of mass, momentum, and energy, which implies an uncomplicated interpretation of the observed response of electrons to an external disturbance. The laws of hydrodynamics become applicable to clean electron systems, where electron-electron collisions with conservation of momentum predominate over scattering of electrons without conservation of momentum (for a review, see Ref. [2]). More explicitly, electron systems reveal collective fluid behavior when the effective Knudsen parameter $\zeta = \tau_{ee}/\tau_p \ll 1$, where τ_{ee} and τ_p are the momentum-conserving electron-electron collision time and momentum-relaxing scattering time, respectively. One of the fundamental properties of hydrodynamic systems is the space-dependent drift velocity which leads to a nonuniform hydrodynamic flow. The nonuniformity of a viscous hydrodynamic systems is manifested itself in a Hagen-Poiseuille flow with a parabolic diffusion velocity profile [3]. Another manifestation of the hydrodynamic nature is the Venturi effect, which is a direct consequence of the mass continuity principle, and it is one of the key concepts in the continuum hydrodynamics of an inviscid fluid. This effect is that the pressure of the fluid decreases and therefore the velocity increases as the fluid flows through the constricted section of the pipe. The Venturi effect has found a vast number of applications. The issue related to the electronic Venturi effect was first discussed in Ref. [4], where the mechanism of quantum pumping in a Fermi system, similar to classical Bernoulli pumping, was considered. Experimental evidence of electronic quantum pumping was obtained in an electron-avalanche amplifier based on a GaAs/AlGaAs heterostructure in Refs. [5,6] and in a graphene field-effect transistor in Ref. [7].

Due to the interplay between momentum-conserving electron-electron and momentum-relaxing electron-phonon scattering, the hydrodynamic electron flow condition is satisfied in a narrow temperature window, typically 4–35 K, where electron viscosity is temperature dependent. In this temperature range, electrons exhibit strong and weak hydrodynamic regimes, in which internal friction and hence shear stress are strong or weak, respectively. In the weak hydrodynamic regime electrons are practically inviscid. The Hagen-Poiseuille diffusion velocity profile is a fundamental characteristic of viscous flow.

To observe the inhomogeneous nature of the electron flow, it is necessary to carry out measurements with spatial resolution. To date, measurements with spatial resolution, which unambiguously testify to the hydrodynamic nature of the electron flow, have been carried out in graphene using a scanning carbon nanotube single-electron transistor [8], nanoscale quantum spin magnetometers [9], scanning tunneling potentiometry [10], in semimetal WTe_2 using a nanoscale scanning superconducting quantum interference device [11], and in the GaAs epilayer using a scanning tunneling microscopy [12].

We recently performed scanning microscopy photocurrent measurements to study the diffusion of holes photoinjected into a high-mobility GaAs quantum well (QW) where the electrons reveal hydrodynamic properties [13,14]. It was found that the observed diffusion consists of the diffusion of heavy and light holes occurring in a viscous electron-hole fluid. In this Letter we address our investigation to the dynamics of diffusion of photogenerated holes in a mesoscopic GaAs

*pusep@ifsc.usp.br

channel of variable width. Using time-resolved photoluminescence scanning microscopy (TRPL), we demonstrate both of the aforementioned hydrodynamic features: the Venturi effect and the paraboliclike velocity profile. Such measurements make it possible to directly investigate the nonuniformity of an electron system, which is one of the most obvious proofs of its hydrodynamic nature. In addition, an unusual increase in the recombination rate with temperature was found, which is analogous to a decrease in the electrical resistance of viscous electrons with temperature.

It is worth noting that according to Ref. [15], in GaAs QWs the effective Knudsen parameter is generically much smaller than unity and "electrons in high-mobility two-dimensional (2D) GaAs are by far the best system for the direct observation of collective hydrodynamic effects conditions for studying electron hydrodynamics."

Experimental details. Here, we studied a single 46-nm-thick GaAs QW, grown on a (100)-oriented GaAs substrate by molecular beam epitaxy. QW barriers were grown in the form of short-period GaAs/AlAs superlattices. The sheet electron density and the mobility measured at a temperature of 1.4 K were $6.7\times10^{11}\text{cm}^{-2}$ and 2.0×10^{6} $\text{cm}^2/\text{V s}$, respectively, using a standard Hall bar structure in Ref. [16], where the viscous character of electron transport was demonstrated in Ref. [16]. Electron hydrodynamics was observed at temperatures above 10 K, at least up to 100 K [17], while the electron-hole fluid exhibits hydrodynamic behavior in the temperature window 4–30 K [13]. The energy structure of the samples studied here is similar to the structure calculated in Ref. [14]. The electric field built in the barriers spatially separates the electrons and holes photogenerated in the barriers. As a result, photogenerated holes tunnel into the quantum well. Holes injected in this way into the GaAs QW lead to the emergence of a multicomponent hydrodynamic fluid formed by background electrons and photogenerated holes. The structure studied here consists of the sections width 4, 10, and 50 μm. The time of recombination of photogenerated holes with background electrons was measured using TRPL in various sections at the emission energy of GaAs QWs. In this work, the same GaAs QW is used to fabricate a mesoscopic channel with section widths of 4, 10, and 50 μm.

Scanning TRPL microscopy experiments were performed at temperatures 4 and 25 K using a helium closed-cycle cryostat equipped with a superconducting magnet (Attocube/Attodry1000). These temperatures were chosen in order to distinguish the effect of electron viscosity. According to Ref. [13], the maximum electron viscosity is expected at 25 K. TRPL measurements with a temporal resolution of 100 ps were made using PicoQuant/LDH Series diode lasers emitting 80 MHz pulses at 730 nm (1.7 eV) and 440 nm (2.82 eV) with a pulse duration of 70 ps. Excitation at 1.7 eV generates electron-hole pairs in the GaAs QW, but not in the barrier, whose gap is about 1.8 eV, while an excitation energy of 2.33 eV leads to electron-hole excitation both in the QW and in the barrier. The electron-hole pairs photogenerated in the QW rapidly recombine and do not contribute to the diffusion. At the same time, holes injected from the barriers form a diffusion flow in the QW channel [14]. Photoluminescence (PL) emission was dispersed by a 75-cm Andor/Shamrock spectrometer and the PL decay transients were detected by a

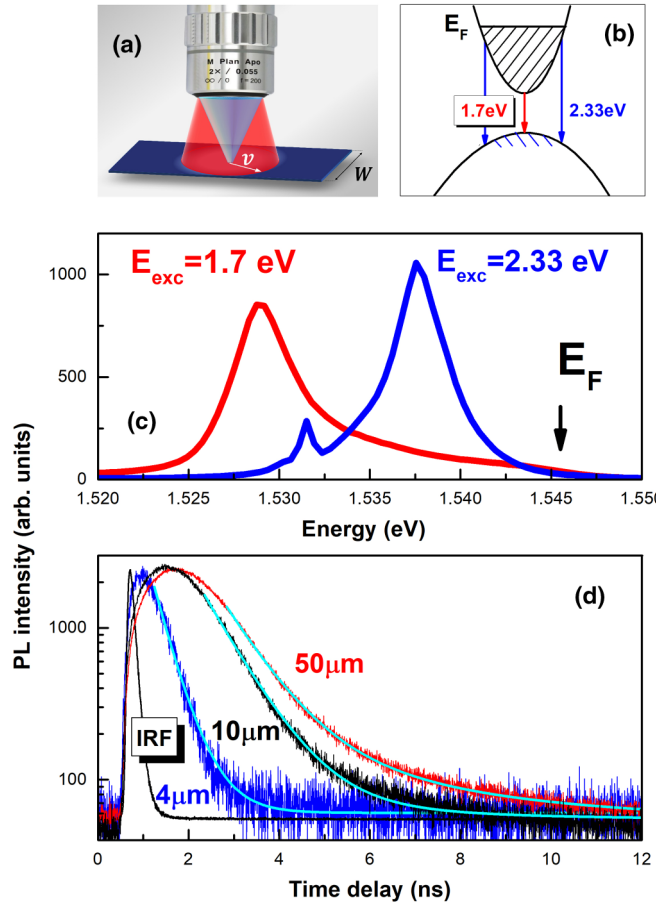

FIG. 1. (a) Sketch of the excitation/collection probe, (b) scheme of PL transitions at different laser excitation energies, (c) typical PL spectra measured at $T = 4$ K and laser excitation at 440 nm (2.33 eV) and 730 nm (1.7 eV) at a pump power of 7.5 μW, and (d) typical PL decay transients measured in channel sections of different widths 4, 10, and 50 μm at $T = 4$ K and laser excitation at 440 nm (2.33 eV); the cyan lines show the results of the best fits.

PicoQuant Hybrid photomultiplier (PMT) detector triggered with a time correlated single photon PicoQuant/PicoHarp 300 counting system. The laser instrument response function (IRF), which is responsible for the temporal resolution of the setup, was measured as a transient process of reflected laser light measured at the laser energy and it is shown in Fig. 1(d). Electron-hole pairs are generated by a laser spot about 1 μm in size. The spatial resolution of the setup is determined by the size of the light collection area, which is estimated at about 10 μm in the spectral range of GaAs QW radiation due to a chromatic aberration.

The scheme of the excitation/collection process is shown in Fig. 1(a). Holes injected into the quantum well at the focus of the lens diffuse to the boundaries of the light collection area at a velocity determined by the properties of the electron-hole fluid. The scheme of PL transitions at laser excitation energies of 1.7 and 2.33 eV and the corresponding PL spectra measured at a pump power of 7.5 μW, which excludes sample heating, are shown in Figs. 1(b) and 1(c), respectively. They demonstrate the effect of hole accumulation in the QW upon excitation at a wavelength of 440 nm. In the *n*-type QW

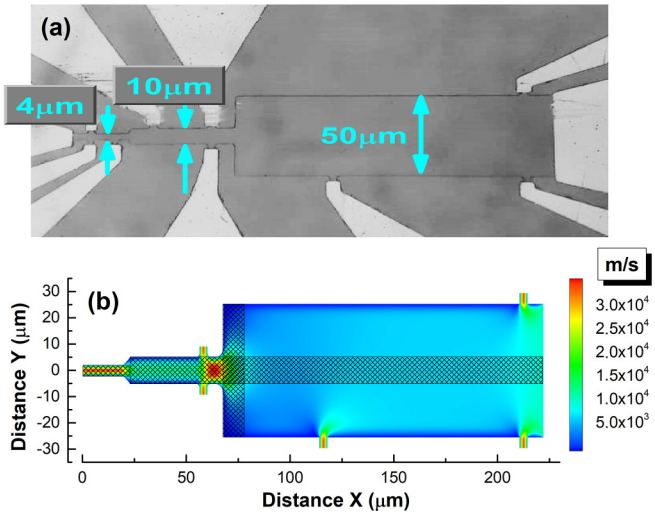

FIG. 2. (a) The sample image and (b) the velocity flow contour plot in a variable-width hydrodynamic channel calculated with the fluid parameters defined in the text. The scanning bands parallel and perpendicular to the channel, determined by the spatial resolution of the PL, are shown as mesh strips.

under study, the shape of the PL spectrum is affected by the occupation of the states of the valence band by minority photogenerated holes. Not all electrons below the Fermi energy contribute equally to recombination with photogenerated holes. Only a small fraction of electrons near the bottom of the conduction band is available for this process, since at low temperatures and low pump powers only a small number of hole states at the top of the valence band are occupied. The shape of the PL spectra measured upon excitation at a wavelength of 730 nm, which generates electron-hole pairs in the GaAs QW, shows that the majority of holes are located at the valence band extremum, which leads to a strong energy maximum near the band edge. At the same time, excitation at a wavelength of 440 nm in the AlGaAs barriers causes the accumulation of holes in the QW, which leads to an increase in the number of high-energy electrons participating in recombination. In this case, the PL maximum shifts towards higher energies, close to the Fermi energy. All experimental data presented below were obtained at a laser pump power of 7.5 μW. The sample image is shown in Fig. 2(a). Holes injected from the laser excitation spot cause a perturbation in the electron hydrodynamic system on the scale of the hole diffusion length. Due to the hydrodynamic properties of the electrons, this perturbation propagates over the entire channel. The diffusion of holes in a system of hydrodynamic electrons can be associated with the diffusion of particles in an incompressible fluid contained in a channel. The stationary flow of such particles injected at any point in the channel creates pressure conditions that depend on the geometry of the channel, which in turn affect the diffusion rate at the point of injection.

Side contacts connect the channel with contact pads, the area of which significantly exceeds the area of the channel. Thus, the contact pads serve as open reservoirs into which photogenerated holes can flow. During measurements, all contacts remained floating and not grounded, while electrons ensure equipotential conditions throughout the entire structure of the sample.

To model the flow of photogenerated holes in this case, the flow of a two-dimensional fluid was calculated by the Navier-Stokes equation using the ANSYS R19.2 code. The parameters required for these calculations were obtained in similar structures in Refs. [13,14]. These include the diffusion coefficient/kinematic viscosity $D_{hh} = \nu_{hh} = 0.17\ \mathrm{m}^2/\mathrm{s}$ and the diffusion length attributed to heavy holes, measured at $T = 25$ K, equal to $L_{hh} = 6$ μm. According to these data the diffusion flow velocity is $v = 3D_{hh}/L_{hh} \simeq 8.5\times10^4$ m/s. When simulating hydrodynamic flow, the contact pins were left open. The corresponding velocity flow contour plot calculated in viscous fluid is shown in Fig. 2(b). As follows from the calculations presented in Fig. 2(b), the diffusion rate increased as the holes entered the narrow contact pins, as would be expected from fluid dynamics.

It is important to note that, taking into account the experimental conditions used, such model calculations provide a qualitative analysis. Nevertheless, even such a simple model is capable of reproducing the essential features of the experiment.

To measure the diffusion velocity of holes, we use the fact that the rate of recombination of photogenerated holes $1/\tau$, where τ is their recombination time with background electrons, is proportional to the flow rate of holes through a certain cross section. In this case the recombination time is given by $\tau = C/v$, where it is assumed that $C = \mathrm{const}$ at a definite laser pump power. The recombination times were obtained by fitting the PL decay transients measured along the scan bands shown in Fig. 2(b).

Results and discussion. The typical transient of PL decay measured at a laser excitation energy of 2.33 eV, at the maxima of the PL spectra along the center line of channel sections of different widths, is shown in Fig. 1(c). The measured PL transients exhibited a mostly monoexponential decay with a characteristic time related to the time of recombination of heavy holes with background electrons. In contrast to the narrow 14-nm QW studied in Refs. [13,14], no presence of light holes was found in such a wide 46-nm QW. In a narrow QW, both heavy and light holes participate in the recombination process, since spatial quantization removes the degeneracy of heavy and light holes at the center of the Brillouin zone. At the same time, in a wide QW, the subbands of heavy and light holes are close to degeneracy, which leads to the predominant recombination of heavy holes due to their higher density of states. The data presented in Fig. 1(d) show that the recombination time decreases with decreasing channel width, indicating a corresponding increase in the diffusion velocity expected from the Venturi effect.

To find hydrodynamic evidence in the diffusion flow of photogenerated holes, the time of their recombination across a wide section of the channel was measured. The corresponding scanning band, along which the maximum change in flow velocity is expected, is shown in Fig. 2(b). The recombination times of photogenerated heavy holes obtained by the monoexponential fitting of the PL transients are depicted in Figs. 3(a) and 3(b) and demonstrate the nonuniform velocity distribution over the channel width, which is expected for a hydrodynamic flow. A significantly stronger change in the recombination

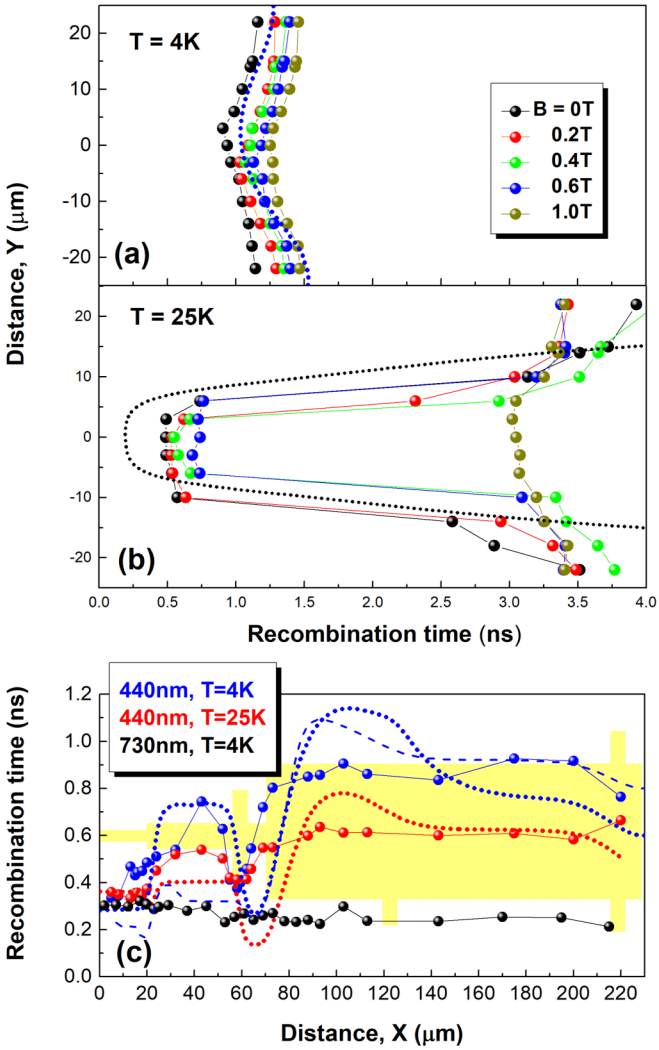

FIG. 3. The recombination time measured (a), (b) perpendicular and (c) parallel to the channel at 4 and 25 K, at an excitation energy of 2.33 eV (440 nm) and in various magnetic fields. Black dotted lines were calculated as described in the text. The recombination time measured parallel to the channel at an excitation energy of 1.7 eV (730 nm) is shown in (c). The measurements were carried out along the strips shown in Fig. 2(b). The dotted lines are the recombination times calculated for inviscid (blue line) and viscous (red line) fluids, and as described in the text. The dashed line in (c) is calculated for 4 K including all contact pins.

time across the channel width is observed at $T = 25$ K compared to $T = 4$ K. This is due to an increase in the viscosity of the electron-hole fluid at $T = 25$ K [13]. An increase in viscosity leads to an increase in internal friction and, as a consequence, to increased energy dissipation. The lower the flow energy, the less its velocity changes when the channel width changes. The velocity profiles calculated for an inviscid and viscous fluid are shown as black dotted lines in Figs. 3(a) and 3(b). They demonstrate inhomogeneous Hagen-Poiseuille profiles and well describe the changes in recombination times observed at $T = 4$ K and $T = 25$ K, respectively.

Furthermore, a magnetic field creates a Lorentz force acting on the hydrodynamic electron-hole fluid, which reduces the effective mean free path and thereby suppresses the viscosity [18,19]. The data shown in Figs. 3(a) and 3(b) indicate that at $T = 4$ K the electron-hole fluid is practically inviscid. In this case, the formation of Landau levels results in a slight increase in the recombination time. At the same time, at $T = 25$ K, when the electron-hole fluid is expected to be viscous, a strong change in the time of recombination indicates a suppression of the viscosity induced by the magnetic field. According to the data presented in Fig. 3(b), a 1 T magnetic field transforms a viscous electron-hole liquid into an inviscid one with a velocity profile similar to that obtained at $T = 4$ K.

The recombination time measured along the channel is depicted in Fig. 3(c). As shown, under the high-energy excitation of 2.33 eV, the recombination time increases with increasing channel width. This is a direct consequence of the Venturi effect: The recombination time is inversely proportional to the flow rate of photogenerated holes, which decreases with increasing channel width. To prove that the observed effect is due to the hydrodynamic flow of holes injected from barriers, we measured the recombination times of holes photogenerated by laser excitation with an energy of 1.7 eV, which creates electron-hole pairs exclusively in the channel. In this case no significant change in the recombination time is found. Thus, unlike holes injected from barriers, electron-hole pairs photogenerated in a channel recombine rapidly and do not form a hydrodynamic flow.

According to the Venturi effect, the flow velocity is inversely proportional to the width of the channel sections. Thus, it is expected that the recombination times measured in different sections will be proportional to the section width and should be scaled as $1 : 2.5 : 12.5$, where 1 corresponds to the section with the minimum width. At the same time, the experimental recombination times are scaled as $1 : 1.8 : 2.3$ at $T = 4$ K and $1 : 1.5 : 1.9$ at $T = 25$ K. It has been found that the presence of potentiometric contacts significantly affects the flow velocity distribution. Adding contact pins considerably reduces the corresponding flow velocity and allows the calculated recombination timescale to be adjusted to the experimental one. The best fits were obtained with contact pins to the middle and wide sections, as shown by the dotted lines in Fig. 3(c). At the same time, the dashed line calculated for an inviscid fluid shows that the addition of contact pins to a narrow section somewhat worsens the agreement between the calculated and experimental recombination times. The observed discrepancy is probably due to the fact that the diffusion length of holes is comparable to the width of the narrow section. In this case the diffusion of holes is remarkably affected by the channel boundary, which changes the flow rate distribution. The effect of channel boundaries on the recombination time of photogenerated holes was studied in Ref. [14], where an optical analog of the Gurzhi effect was observed.

It should be noted that when calculating the flow rates and the corresponding recombination times, no fitting parameters were used, except for the constant C, which determines the relationship between the flow rate and the recombination time and was taken equal to 6000 and 4500 m for $T = 4$ K (inviscid flow) and 25 K (viscous flow), respectively. Nevertheless, all the observed experimental features of the recombination time are well reproduced. This demonstrates the reliability of the model used.

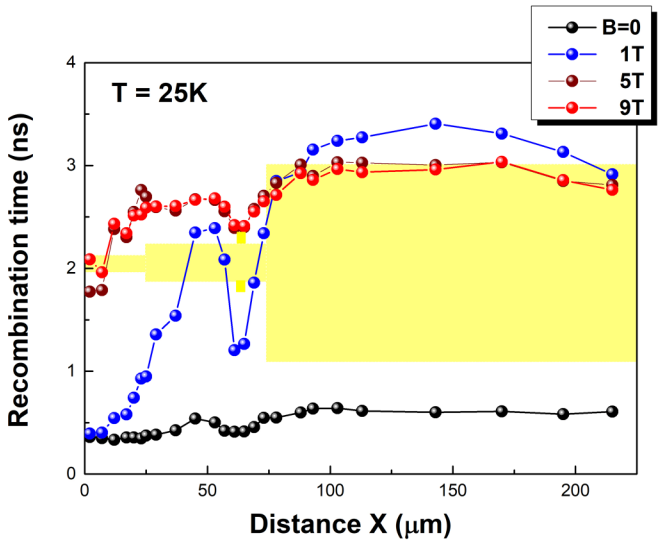

FIG. 4. The recombination times measured along the channel at 25 K in various magnetic fields.

The decrease in recombination time with temperature, shown in Fig. 3(c), is associated with a change in the nature of the electron-hole fluid from inviscid to viscous. The effect of temperature is more pronounced in the wide section, and insignificant in the narrow one. The change in the recombination time is associated with a change in the mean free path and, consequently, with a change in the diffusion length L. The diffusion length of heavy holes as a function of temperature was measured in a similar sample in Ref. [13]. Using these data, we compare the effect of temperature on the viscosity of an electron-hole fluid observed by different independent methods. By using the Einstein relation $D = \mu E_F/\mathrm{e}$, where μ is the mobility, and the diffusion coefficient $D = L^2/\tau$, the recombination time can be expressed as

$$\tau = \frac{\mu E_F}{eL^2}. \tag{1}$$

If we assume that in the considered temperature range the mobility remains unchanged, then the change in the recombination time is related to the diffusion length. The diffusion lengths of heavy holes measured in Ref. [13] are 4 and 7 μm at 4 and 25 K, respectively. Application of Eq. (1) to an electron-heavy hole fluid gives a recombination time at 4 K that is three times longer than at 25 K, which somewhat exceeds the change by 1.4 times observed in the wide section. However, in a viscous fluid, mobility that increases with increasing temperature can improve the agreement between calculated and measured recombination times. In a narrow section, diffusion is limited by its width and, therefore, does not depend noticeably on temperature.

In addition, the effect of the magnetic field on the distribution of velocities along the channel, shown in Fig. 4, again reflects the influence of the magnetic field on the viscosity of the electron-hole fluid. As shown in Fig. 3(c), the difference in recombination times measured in channel regions of different widths increases with decreasing viscosity. A similar increase in the recombination time was found with increasing magnetic field. In the 4-μm-wide section of the channel, due to the higher diffusion velocity, the effect of the magnetic field on viscosity is achieved at a stronger magnetic field than in wide sections. In the 4-μm-wide section of the channel, due to the higher diffusion velocity, the effect of the magnetic field on viscosity is achieved at a stronger magnetic field than in wide sections. Taking into account the phenomenological character of the model used to calculate the flow velocity distribution in the channel, a good agreement was found between the experimental and calculated recombination times. This proves the hydrodynamic nature of the diffusion of photogenerated holes in the sample studied here. Despite its simplicity, the model used reproduces the main experimental features, such as change in the recombination time in sections of different widths and across the channel, and change in the recombination time with a change in viscosity. Model calculations reproduce even the minimum of the recombination time observed at the point where the channel width changes.

Conclusion. In summary, to study the diffusion of holes in a hydrodynamic electron system, another method for determining the diffusion velocity was used, which consists in measuring the recombination rate of photogenerated holes. Accordingly, TRPL scanning with micrometer resolution was performed in a mesoscopic variable-width GaAs channel, where the hydrodynamic features of the electron-hole fluid, such as the Venturi effect and the parabolic Hagen-Poiseuille velocity profile, are demonstrated. The observed decrease in the recombination time with increasing temperature is unusual and indicates the viscous nature of the investigated electron-hole fluid. This effect is similar to the decrease in the electrical resistance of viscous electrons with increasing temperature. Moreover, a magnetic-field-induced suppression of viscosity is observed. The presented results manifest to the fundamental role of viscosity in the hydrodynamic flow of an electron-hole fluid in the GaAs mesoscopic channel under study.

Acknowledgment. Financial support from the Brazilian agencies FAPESP (Grants No. 2021/12470-8, No. 2022/02132-0, and No. 2022/10340-2) and CAPES (Grant No. PNPD 88887.336083/2019-00) is gratefully acknowledged.

[1] M. Polini and A. K. Geim, Viscous electron fluids, Phys. Today **73** (6), 28 (2020).

[2] L. Fritz and T. Scaffidi, Hydrodynamic electronic transport, arXiv:2303.14205.

[3] F. M. White, *Fluid Dynamics* (McGraw Hill, New York, 2009).

[4] A. O. Govorov and J. J. Heremans, Hydrodynamic effects in interacting Fermi electron jets, Phys. Rev. Lett. **92**, 026803 (2004).

[5] D. Taubert, G. J. Schinner, H. P. Tranitz, W. Wegscheider, C. Tomaras, S. Kehrein, and S. Ludwig, Electron-avalanche amplifier based on the electronic Venturi effect, Phys. Rev. B **82**, 161416(R) (2010).

[6] D. Taubert, G. J. Schinner, C. Tomaras, H. P. Tranitz, W. Wegscheider, and S. Ludwig, An electron jet pump: The Venturi effect of a Fermi liquid, J. Appl. Phys. **109**, 102412 (2011).

[7] W. Huang, T. Paul, K. Watanabe, T. Taniguchi, M. L. Perrin, and M. Calame, Electronic Poiseuille flow in hexagonal boron nitride encapsulated graphene field effect transistors, Phys. Rev. Res. **5**, 023075 (2023).

[8] J. A. Sulpizio, L. Ella, A. Rozen, J. Birkbeck, D. J. Perello, D. Dutta, M. Ben-Shalom, T. Taniguchi, K. Watanabe, T. Holder, R. Queiroz, A. Principi, A. Stern, T. Scaffidi, A. K. Geim, and S. Ilani, Visualizing Poiseuille flow of hydrodynamic electrons, Nature (London) **576**, 75 (2019).

[9] M. J. H. Ku, T. X. Zhou, Q. Li, Y. J. Shin, J. K. Shi, C. Burch, L. E. Anderson, A. T. Pierce, Y. Xie, A. Hamo, U. Vool, H. Zhang, F. Casola, T. Taniguchi, K. Watanabe, M. M. Fogler, P. Kim, A. Yacoby, and R. L. Walsworth, Imaging viscous flow of the Dirac fluid in graphene, Nature (London) **583**, 537 (2020).

[10] Z. J. Krebs, W. A. Behn, S. Li, K. J. Smith, K. Watanabe, T. Taniguchi, A. Levchenko, and V. W. Brar, Imaging the breaking of electrostatic dams in graphene for ballistic and viscous fluids, Science **379**, 671 (2023).

[11] A. Aharon-Steinberg, T. Völkl, A. Kaplan, A. K. Pariari, I. Roy, T. Holder, Y. Wolf, A. Y. Meltzer, Y. Myasoedov, M. E. Huber, B. Yan, G. Falkovich, L. S. Levitov, M. Hücker, and E. Zeldov, Direct observation of vortices in an electron fluid, Nature (London) **607**, 74 (2022).

[12] B. A. Braem, F. M. D. Pellegrino, A. Principi, M. Röösli, C. Gold, S. Hennel, J. V. Koski, M. Berl, W. Dietsche, W. Wegscheider, M. Polini, T. Ihn, and K. Ensslin, Scanning gate microscopy in a viscous electron fluid, Phys. Rev. B **98**, 241304(R) (2018).

[13] Y. A. Pusep, M. D. Teodoro, V. Laurindo, Jr., E. R. C. de Oliveira, G. M. Gusev, and A. K. Bakarov, Diffusion of photoexcited holes in a viscous electron fluid, Phys. Rev. Lett. **128**, 136801 (2022).

[14] Yu. A. Pusep, M. D. Teodoro, M. A. T. Patricio, G. M. Jacobsen, G. M. Gusev, A. D. Levin, and A. K. Bakarov, Dynamics of recombination in viscous electron–hole plasma in a mesoscopic GaAs channel, J. Phys. D: Appl. Phys. **56**, 175301 (2023).

[15] S. Ahn and S. Das Sarma, Hydrodynamics, viscous electron fluid, and Wiedeman-Franz law in two-dimensional semiconductors, Phys. Rev. B **106**, L081303 (2022).

[16] G. M. Gusev, A. S. Jaroshevich, A. D. Levin, Z. D. Kvon, and A. K. Bakarov, Viscous magnetotransport and Gurzhi effect in bilayer electron system, Phys. Rev. B **103**, 075303 (2021).

[17] A. D. Levin, G. M. Gusev, A. S. Yaroshevich, Z. D. Kvon, and A. K. Bakarov, Geometric engineering of viscous magnetotransport in a two-dimensional electron system, Phys. Rev. B **108**, 115310 (2023).

[18] M. S. Steinberg, Viscosity of the electron gas in metals, Phys. Rev. **109**, 1486 (1958).

[19] P. S. Alekseev, Negative magnetoresistance in viscous flow of two-dimensional electrons, Phys. Rev. Lett. **117**, 166601 (2016).